International Journal of Applied Mathematics

Volume 28 No. 1 2015, 65-84
ISSN: 1311-1728 (printed version); ISSN: 1314-8060 (on-line version)
doi: http://dx.doi.org/10.12732/ijam.v28i1.6

A FINITE VOLUME METHOD TO SOLVE THE COMPRESSIBLE NAVIER-STOKES SYSTEM ON UNSTRUCTURED MESH

Rabé Badé[1] §, Hedia Chaker[2], Mohamed Abdelwahed[3]

[1]Département de Mathématiques et Informatique
Faculté des Sciences et Techniques
Université Abdou Moumouni
BP 10662, Niamey, NIGER
[2]Ecole Nationale d'Ingénieurs de Tunis
LAMSIN, BP 37, Tunis, TUNISIA
[3]Department of Mathematics
College of Sciences
King Saud University, Riyadh, SAUDI ARABIA

Abstract: This work is devoted to the numerical solution of the three dimensional (3D) compressible Navier-Stokes system on unstructured mesh. The numerical simulation are performed using a fractional step method treating separately the convection and the diffusion parts. The discretization is done by the finite volume method for the two parts. The convective flux is computed by the Godunov method and a new scheme is presented for the treatment of the diffusive flux. The technique is illustrated by solving various numerical problems.

AMS Subject Classification: 65M08, 35Q30, 35Q31
Key Words: fractional step method, finite volume method, hyperbolic system, Riemann problem

Received: November 25, 2014
© 2015 Academic Publications
§Correspondence author

1. Introduction

The Navier-Stokes equations are used to describe various fluids flows in nature such as: shallow water, in aerodynamic, in hydrodynamic, in meteorology, etc. For this reason, different numerical methods are developed with the aim to reproduce or predict the physics of the phenomenon. Among these methods we can cite: the finite element method: Girault et al. [14], Glowinski et al. [15] and Temam [26], the spectral method: Bernardi et al. [4], Hussaini et al. [16] and Minev et al. [22] and the finite volume method: Boivin et al. [5] and Boivin et al. [6]. In this work we are interested in the finite volume method which is particularly popular due to its conservative nature. In any case, one of the major difficulties to solve the compressible Navier-Stokes equations for a viscous fluid is the non-linearity which appears in the convective term. Different methods are used to treat this non-linearity like the characteristics' method see Pironneau et al [23] or the two-grid scheme in Abboud et al. [1]. But the most traditional approach to overcome this difficulty is the fractional time step method: Chorin [7], Temam [25] and Boivin et al. [6]. In general, the differential operators admit a decomposition into a sum of components of simple structure. This observation is the key issue in the operator splitting approach, since the operator components can be treated separately rather than simultaneously. So our splitting is based on a separation of the physical phenomena which interact in the compressible Navier-Stokes equations, in occurrence the convection and the diffusion in order to use convenient method for each part. The Godunov method is applied for the convective flux. For the diffusive part, different schemes can be used. The cell-centred finite volume scheme is widely used in fluid dynamics community: Boivin et al. [5], Boivin et al. [6], Eymard et al. [10] and [11] and are largely considered in commercial codes. But the major disadvantage of this scheme is that it can be applied only on orthogonal meshs. In Komla et al. [8] and Manzini et al. [21] this constraint has been overcome by considering a dual mesh based on diamond cells built from cells centroid of the primal mesh. This approach remains computationally efficient in 2D but in 3D the complexity becomes easily out of control.

A new scheme is presented in this work to compute the gradient and divergence on the cell interfaces. In our approach, we use cells surrounding the interface on which we want to approach the flux without considering another mesh. This allows us to evaluate the interfacial gradient and divergence using simply the discrete unknowns in the considered cells and a simple change between the canonical basis and a new basis built from the centroids of the surrounding cells.

The paper is organized as follows. We first recall the compressible Navier-Stokes equations and we present the convection and the diffusion parts obtained by using the fractional step method. Then we present in Section 3 how we compute respectively the convective and the diffusive flux obtained from the finite volume discretization. Finally, Section 4 is devoted to the validation tests, first for every part separately and secondly for the complete system.

2. Governing Equations

The Navier-Stokes equations for compressible viscous fluids are given by:

$$\begin{cases} \dfrac{\partial \rho}{\partial t} + \nabla \cdot (\rho \mathbf{u}) = 0, \\ \dfrac{\partial \rho \mathbf{u}}{\partial t} + \nabla \cdot (\rho \mathbf{u} \otimes \mathbf{u}) - \mu \triangle \mathbf{u} - (\dfrac{\mu}{3} + \lambda) \nabla (\nabla \cdot \mathbf{u}) + \nabla p = \mathbf{f}, \\ \dfrac{\partial \rho E}{\partial t} + \nabla \cdot \big((\rho E + p) \mathbf{u} \big) = -\nabla \cdot \mathbf{q} - \nabla \cdot \big(\sigma \mathbf{u} \big) + \mathbf{u} \cdot \mathbf{f}, \end{cases} \tag{1}$$

where ρ, $\mathbf{u}$=(u_1, u_2, u_3), $E = e + \frac{\|\mathbf{u}\|^2}{2}$, p, $\sigma = \mu\big(\nabla \mathbf{u} + \nabla \mathbf{u}^T\big) - \big(\lambda - \frac{2}{3}\mu\big)\mathbf{I_d} \nabla \cdot \mathbf{u}$ and $\mathbf{f}$ denote respectively the density, the velocity components, the total energy, the pressure, the stress tensor and the external forces. μ and λ are the dynamic and compression viscosities. System (1) is closed by considering the following state law (see Abgrall et al. [2] and Andrainov et al. [3]):

$$P(\rho, e) = (\gamma - 1)\rho e - \gamma P_\infty \ , \qquad e(\rho, \theta) = P_\infty / \rho + C_v \theta \cdot \tag{2}$$

Here γ and P_∞ are given constants depending on the fluid (air: $\gamma = 1.4$, $P_\infty = 0$, water: $\gamma = 5.5$, $P_\infty = 407.10^6$), C_v is the calorific capacity with constant volume and θ is the temperature. Moreover, the system (1) is completed by the initial condition and boundary conditions. To solve numerically the system (1), we use the fractional step method. It consists to treat the convective and diffusion parts while preserving the interaction between them with well appropriate initial conditions. This amounts to trait:

First step: Convection part

$$\begin{cases} \dfrac{\partial \rho}{\partial t} + \nabla \cdot (\rho \mathbf{u}) = 0, \\ \dfrac{\partial \rho \mathbf{u}}{\partial t} + \nabla \cdot (\rho \mathbf{u} \otimes \mathbf{u}) + \nabla p = 0, \\ \dfrac{\partial \rho E}{\partial t} + \nabla \cdot \left(\big(\rho E + p \big) \mathbf{u} \right) = 0. \end{cases} \tag{3}$$

Second step: Duffision part
In this step we use the Fourier law and the internal energy state law (2), to get the momentum diffusion

$$\begin{cases} \dfrac{\partial \rho}{\partial t} = 0, \\ \rho \dfrac{\partial \mathbf{u}}{\partial t} - \mu \triangle \mathbf{u} - (\dfrac{\mu}{3} + \lambda)\nabla(\nabla \cdot \mathbf{u}) = \mathbf{f}, \end{cases} \tag{4}$$

and the heat diffusion

$$\rho C_v \frac{\partial \theta}{\partial t} - k \triangle \theta = \big(\lambda - \frac{2}{3}\mu\big)|\nabla \cdot \mathbf{u}|^2 + \frac{\mu}{2}|\nabla \mathbf{u} + \nabla \mathbf{u}^T|^2. \tag{5}$$

3. Numerical Discretization

The numerical discretization of all parts is done using the finite volume method, so the physical domain is discretized to from disjoint hexahedrons named cell and denoted by M_i. Let us denote by $\triangle t$ the time step discretization, and for any continuous variable $c(x,t)$, c_i^n represent the discrete variable in M_i at time $t^n = n\triangle t$. At $t = 0$ we consider c_i^0 as the average value of the initial condition in each M_i. The discrete systems are obtained by integrating on $[t^n, t^{n+1}] \times M_i$. Now we assume that: ρ_i^n, $\mathbf{u}_i^n$, p_i^n and θ_i^n are given. In the first step we solve the convection part. The numerical solutions denoted by $\rho_i^{n+\frac{1}{2}}$, $\mathbf{u}_i^{n+\frac{1}{2}}$, $p_i^{n+\frac{1}{2}}$ and $E_i^{n+\frac{1}{2}}$ are computed by the following discrete system:

$$\begin{aligned} \rho_i^{n+\frac{1}{2}} &= \rho_i^n - \tfrac{1}{|M_i|} \sum_{\sigma_{ij} \in \partial M_i} \int_{t^n}^{t^{n+1}} \int_{\sigma_{ij}} \rho_{ij} \mathbf{u}_{ij} \cdot \mathbf{n}_{ij} d\Gamma dt, \\ \rho_i^{n+\frac{1}{2}} \mathbf{u}_i^{n+\frac{1}{2}} &= \rho_i^n \mathbf{u}_i^n - \tfrac{1}{|M_i|} \sum_{\sigma_{ij} \in \partial M_i} \int_{t^n}^{t^{n+1}} \int_{\sigma_{ij}} (\rho_{ij}(\mathbf{u}_{ij} \cdot \mathbf{u}_{ij}) \cdot \mathbf{n}_{ij} + p_{ij} \cdot \mathbf{n}_{ij}) d\Gamma dt, \\ \rho_i^{n+\frac{1}{2}} E_i^{n+\frac{1}{2}} &= \rho_i^n E_i^n - \tfrac{1}{|M_i|} \sum_{\sigma_{ij} \in \partial M_i} \int_{t^n}^{t^{n+1}} \int_{\sigma_{ij}} (\rho_{ij} E_{ij} + p_{ij}) \mathbf{u}_{ij} \cdot \mathbf{n}_{ij} d\Gamma dt, \end{aligned} \tag{6}$$

where ρ_{ij}, $\mathbf{u}_{ij}$, E_{ij} and p_{ij} represent the values of ρ, $\mathbf{u}$, E and p on the interface σ_{ij} and $\mathbf{n}_{ij}$ is the corresponding outward unit normal vector. $|M_i|$ is the measure of M_i.

In the second step we solve the diffusion part; as initial conditions we take: $\rho_i^{n+\frac{1}{2}}$, $\mathbf{u}_i^{n+\frac{1}{2}}$ for the system (4) and $\theta_i^{n+\frac{1}{2}} = \frac{1}{C_v}(E_i^{n+\frac{1}{2}} - \frac{\|\mathbf{u}_i^{n+\frac{1}{2}}\|^2}{2}) - \frac{P_\infty}{C_v \rho_i^{n+\frac{1}{2}}}$ for the system (5). Finally we compute ρ_i^{n+1}, $\mathbf{u}_i^{n+1}$, p_i^{n+1} and θ_i^{n+1} by:

$$\begin{aligned} &\rho_i^{n+1} = \rho_i^{n+\frac{1}{2}}, \\ &\rho_i^{n+1}\mathbf{u}_i^{n+1} - (\tfrac{\mu}{3}+\lambda) \sum_{\sigma_{ij}\in\partial M_i} \int_{t^n}^{t^{n+1}} \int_{\sigma_{ij}} (\nabla \cdot \mathbf{u_i^{n+1}}) \cdot \mathbf{n}_{ij} d\Gamma \\ &\qquad -\mu \sum_{\sigma_{ij}\in\partial M_i} \int_{t^n}^{t^{n+1}} \int_{\sigma_{ij}} (\nabla \mathbf{u_i^{n+1}} \cdot \mathbf{n}_{ij}) d\Gamma = \rho \mathbf{u}_i^{n+\frac{1}{2}} + \mathbf{f}_i^{n+1}, \end{aligned} \tag{7}$$

$$\begin{aligned} C_v \rho_i^{n+1}\theta_i^{n+1} - k \sum_{\sigma_{ij}\in\partial M_i} \int_{t^n}^{t^{n+1}} \int_{\sigma_{ij}} (\nabla \theta_i^{n+1} \cdot \mathbf{n}_{ij}) d\Gamma = C_v \rho_i^{n+1}\theta_i^{n+\frac{1}{2}} \\ + \big(\lambda - \frac{2}{3}\mu\big)|\nabla \cdot \mathbf{u}_i^{n+1}|^2 + \frac{\mu}{2}|\nabla \mathbf{u}_i^{n+1} + \nabla \mathbf{u}_i^{n+1^T}|^2. \end{aligned} \tag{8}$$

One of the key points of the discretization method using the finite volume is the calculation of interfacial flux. This will be done in our case for the systems (6), (7) and (8) in the following subsections.

3.1. Convective Flux

Calculating the convective flux in the system (6) is to determine the values of ρ_{ij}, $\mathbf{u}_{ij}$, E_{ij} and p_{ij}. Using the fact that:

- the flux depends on the variation of the discrete solutions in the normal direction $\mathbf{n}_{ij}$,
- the rotation invariance of the Euler equations (see Edwige et al. [9] and Toro [27]),
- the discrete unknown being constant by cell,

we can decompose the velocity, in the aim to compute the normal velocity u_η together with ρ_{ij} and p_{ij} by solving the system:

$$\begin{cases} \dfrac{\partial \mathbf{W}}{\partial t} + \dfrac{\partial \mathbf{F}(\mathbf{W})}{\partial \eta} = 0, \\ \mathbf{W}(\eta, 0) = \begin{cases} (\rho_i,\ \rho_i \mathbf{u}_i \cdot \mathbf{n}_{ij},\ \rho_i E_i) & \text{if} \quad \eta < 0, \\ (\rho_j,\ \rho_j \mathbf{u}_j \cdot \mathbf{n}_{ij},\ \rho_j E_j) & \text{if} \quad \eta > 0, \end{cases} \end{cases} \tag{9}$$

with: $\mathbf{W} = (\rho_{ij}, \rho_{ij}u_\eta, \rho_{ij}E_{ij})^T$, $\mathbf{F}(\mathbf{W}) = (\rho_{ij}u_\eta,\ \rho_{ij}u_\eta^2 + p_{ij},\ \rho_{ij}E_{ij})^T$.

Knowing u_η, the tangential components of the velocity u_ζ and u_ν (in the plane containning the interface σ_{ij}) are solutions of:

$$\begin{cases} \dfrac{\partial u_\zeta}{\partial t} + u_\eta \dfrac{\partial u_\zeta}{\partial \eta} = 0, \\ \\ u_\zeta(\eta,\ 0) = \begin{cases} \mathbf{u}_i \cdot \tau_1 & \text{if } \eta < 0, \\ \mathbf{u}_j \cdot \tau_1 & \text{if } \eta > 0, \end{cases} \end{cases} \quad \begin{cases} \dfrac{\partial u_\nu}{\partial t} + u_\eta \dfrac{\partial u_\nu}{\partial \eta} = 0, \\ \\ u_\nu(\eta,\ 0) = \begin{cases} \mathbf{u}_i \cdot \tau_2 & \text{if } \eta < 0, \\ \mathbf{u}_j \cdot \tau_2 & \text{if } \eta > 0. \end{cases} \end{cases} \tag{10}$$

Here the vectors τ_1 and τ_2 generate the plane containning σ_{ij}. In the systems (9) and (10); ρ_i, $\mathbf{u}_i$, p_i (respectively ρ_j, $\mathbf{u}_j$, p_j) are the density, the velocity and the pressure in M_i (respectively in M_j) on both sides of the interface σ_{ij}. Finally the velocity on the interface is $\mathbf{u}_{ij} = (u_\eta, u_\zeta, u_\nu)$.

It remains to solve the systems (9) and (10). As the system (9) is strictly hyperbolic, its solution is composed of three waves separated by four constant states. The 1-wave and the 3-wave are genuinely nonlinear and the 2-wave is linearly degenerate. The entropic solution of the 1D Riemann problem (9) is largely studied in the case of a perfect gas: Edwige et al. [9], Lax [20] and Serre [24]. An extension is presented in this work by considering the more general law (2) which can be applied for a very large kind of fluids. Under the Lax condition and considering the solution of (9) in the phase space, we deduce the following expressions of the different waves:

1-Wave

$$\begin{cases} u_S^1(p) &= u_l - \sqrt{\dfrac{2}{\rho_l}} \sqrt{\dfrac{(p-p_l)^2}{(\gamma+1)p + (\gamma-1)p_l + 2\gamma P_\infty}} & p > p_l, \\ \\ u_R^1(p) &= u_l + \dfrac{2}{\gamma - 1}\sqrt{\dfrac{\gamma}{\rho_l}}\left(\sqrt{p_l + P_\infty} - \sqrt{p + P_\infty}\left(\dfrac{p_l + P_\infty}{p + P_\infty}\right)^{\dfrac{1}{2\gamma}}\right) & p < p_l, \end{cases}$$

3-Wave

$$\begin{cases} u_S^3(p) &= u_r + \sqrt{\dfrac{2}{\rho_r}} \sqrt{\dfrac{(p-p_r)^2}{(\gamma+1)p + (\gamma-1)p_r + 2\gamma P_\infty}} & p > p_r, \\ \\ u_R^3(p) &= u_r - \dfrac{2}{\gamma - 1}\sqrt{\dfrac{\gamma}{\rho_r}}\left(\sqrt{p_r + P_\infty} - \sqrt{p + P_\infty}\left(\dfrac{p_r + P_\infty}{p + P_\infty}\right)^{\dfrac{1}{2\gamma}}\right) & p < p_r, \end{cases}$$

2-contact discontinuity

$$\begin{cases} [u] = 0, \\ [p] = 0, \end{cases}$$

where $\rho_l = \rho_i$, $\rho_r = \rho_j$, $u_l = \mathbf{u}_i \cdot \mathbf{n_{ij}}$, $u_r = \mathbf{u}_j \cdot \mathbf{n_{ij}}$, $p_l = p_i$, $p_r = p_j$ and $[\,]$ represents the jump.

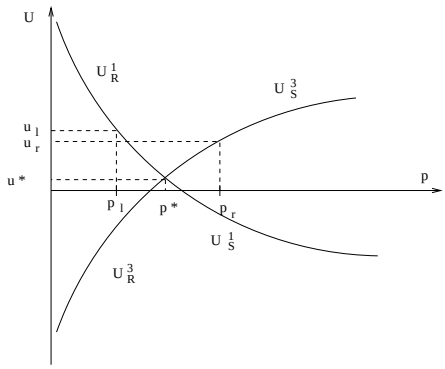

Figure 1: The solution of the Riemann problem in the phases space (p, u).

The intermediate values u^*, p^* are deduced from the intersection between the 1-wave and the 3-wave as shown in Figure 1. ρ_1^* and ρ_2^* are given by:

$$\rho_1^* = \begin{cases} \rho_l \left(\dfrac{p^* + P_\infty}{p_l + P_\infty} \right)^{\frac{1}{\gamma}} & \text{1-rarefaction,} \\ \rho_l \dfrac{(\gamma+1)p^* + (\gamma-1)p_l + 2\gamma P_\infty}{(\gamma-1)p^* + (\gamma+1)p_l + 2\gamma P_\infty} & \text{1-shock.} \end{cases}$$

$$\rho_2^* = \begin{cases} \rho_r \left(\dfrac{p^* + P_\infty}{p_r + P_\infty} \right)^{\frac{1}{\gamma}} & \text{3-rarefaction,} \\ \rho_r \dfrac{(\gamma+1)p^* + (\gamma-1)p_r + 2\gamma P_\infty}{(\gamma-1)p^* + (\gamma+1)p_r + 2\gamma P_\infty} & \text{3-shock.} \end{cases}$$

Using the exact solution of the 1D Riemann problem (9), we obtain ρ_{ij}, u_η and p_{ij} in the normal direction. Thereafter the solutions of the system (10) are computed as follow:

$$u_\zeta = \begin{cases} \mathbf{u}_i \cdot \tau_1 \;\text{ if }\; u_\eta > 0, \\ \mathbf{u}_j \cdot \tau_1 \;\text{ if }\; u_\eta < 0, \end{cases} \quad \text{and} \quad u_\nu = \begin{cases} \mathbf{u}_i \cdot \tau_2 \;\text{ if }\; u_\eta > 0, \\ \mathbf{u}_j \cdot \tau_2 \;\text{ if }\; u_\eta < 0. \end{cases} \tag{11}$$

Boundary Conditions

The 1D Riemann problem (9) is established in the case of an internal interface, in other words, if the datum are known on both sides of the interface. For a boundary interface the flux is computed in another way. The ghost cells method presented in Kirkkörrü et al [18] consists to build a mirror state according to the left state available and the boundary condition imposed on the edge, it allows to have a complete Riemann problem. In the present work we solve the half Riemann problem, which is considered as a Cauchy problem, for which the initial datum is the only discrete unknown in the cell M_i and the boundary condition.

3.2. Diffusive Flux

The diffusive flux in systems (7) and (8) is determined by approximating the gradient and divergence at the interface. For an orthogonal mesh this flux is computed using the cell-centred finite volume scheme like in Boivin et al [5] and Boivin et al. [6].

If this condition is not satisfied, a solution is presented in 2D case by Faille [12]. It consists in considering always the two adjacent cells and creating inside them two points such that the line connecting the new points is orthogonal to σ_{ij} and then applies the centered finite difference scheme using an interpolation of the unknown at these creating points. In 3D, the different possibilities of interpolation make this scheme not useful. In our approach, we build a new basis in which the approximation of the interfacial gradient and divergence is possible by the centered finite differences. Thus as first vector of this basis we take $\overrightarrow{\mathbf{X}_i\mathbf{X}_j}$. We supplement this vector by two others vectors $\overrightarrow{\mathbf{X}_a\mathbf{X}_b}$ and $\overrightarrow{\mathbf{X}_c\mathbf{X}_d}$ where $\mathbf{X}_a$, $\mathbf{X}_b$, $\mathbf{X}_c$, $\mathbf{X}_d$ are artificial points computed respectively as mid-point of the centroids of the two cells which are at the top, in the lower part, in front and behind the interface on which we want to approach the flux (see Figure 2)

$$\mathbf{X}_a = \frac{\mathbf{X}_3+\mathbf{X}_6}{2}, \quad \mathbf{X}_b = \frac{\mathbf{X}_4+\mathbf{X}_5}{2}, \quad \mathbf{X}_c = \frac{\mathbf{X}_9+\mathbf{X}_{10}}{2}, \quad \mathbf{X}_d = \frac{\mathbf{X}_7+\mathbf{X}_8}{2}.$$

Then the interfacial gradient and divergence are computed in this new basis and finally projected onto the normal direction. The obtained approximations

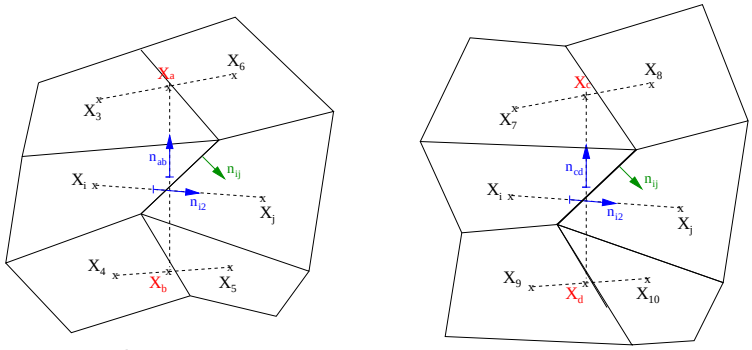

Figure 2: Construction of the points

are given by (12), (13) and (14)

$$(\nabla \mathbf{u} \cdot \mathbf{n}_{ij})^k \approx \sum_{l=1}^{3} \mathcal{P}_{kl} \Bigg(\frac{\mathbf{u}_j^k - \mathbf{u}_i^k}{D_{i.j}} [\mathcal{P}^{-1}]_1 \cdot \mathbf{n}_{ij} + \frac{\mathbf{u}_a^k - \mathbf{u}_b^k}{D_{a.b}} [\mathcal{P}^{-1}]_2 \cdot \mathbf{n}_{ij} + \frac{\mathbf{u}_c^k - \mathbf{u}_d^k}{D_{c.d}} [\mathcal{P}^{-1}]_3 \cdot \mathbf{n}_{ij} \Bigg), \tag{12}$$

$$(\nabla \cdot \mathbf{u}) \cdot \mathbf{n}_{ij} \approx \frac{\mathbf{u}_j^1 - \mathbf{u}_i^1}{D_{i.j}} \mathbf{n}_{ij} + \frac{\mathbf{u}_a^2 - \mathbf{u}_b^2}{D_{a.b}} \mathbf{n}_{ij} + \frac{\mathbf{u}_c^3 - \mathbf{u}_d^3}{D_{c.d}} \mathbf{n}_{ij}, \tag{13}$$

$$\nabla \theta \cdot \mathbf{n}_{ij} \approx \frac{\theta_j - \theta_i}{D_{i.j}} [\mathcal{P}^{-1}]_1 \cdot \mathbf{n}_{ij} + \frac{\theta_a - \theta_b}{D_{a.b}} [\mathcal{P}^{-1}]_2 \cdot \mathbf{n}_{ij} + \frac{\theta_c - \theta_d}{D_{c.d}} [\mathcal{P}^{-1}]_3 \cdot \mathbf{n}_{ij}, \tag{14}$$

where $\mathcal{P}$ is the matrix whose columns are $\overrightarrow{\mathbf{X}_i\mathbf{X}_j}$, $\overrightarrow{\mathbf{X}_a\mathbf{X}_b}$ and $\overrightarrow{\mathbf{X}_c\mathbf{X}_d}$, $[\mathcal{P}^{-1}]_l$ is the l^{th} row of the matrix $\mathcal{P}^{-1}$, $\mathbf{u}^k$ the k^{th} component of $\mathbf{u}$. $\mathbf{u}_a$, $\mathbf{u}_b$, $\mathbf{u}_c$ and $\mathbf{u}_d$ are values of $\mathbf{u}$ at the points $\mathbf{X}_a$, $\mathbf{X}_b$, $\mathbf{X}_c$, $\mathbf{X}_d$ given by:

$$\mathbf{u}_a = \tfrac{\mathbf{u}_3+\mathbf{u}_6}{2}, \quad \mathbf{u}_b = \tfrac{\mathbf{u}_4+\mathbf{u}_5}{2}, \quad \mathbf{u}_c = \tfrac{\mathbf{u}_9+\mathbf{u}_{10}}{2}, \quad \mathbf{u}_d = \tfrac{\mathbf{u}_7+\mathbf{u}_8}{2}.$$

The temperatures θ_a, θ_b, θ_c and θ_d are computed in the same manner. Finally, $D_{i.j} = d(X_i, X_j)$, $D_{a.b} = d(X_a, X_b)$ and $D_{c.d} = d(X_c, X_d)$ ($d(\cdot,\ \cdot)$ is the distance).

Boundary Cell Treatment

In this part we will discuss the case of a cell having one or more of its faces on the boundary. According to its position, two cases arise: first the cell has a neighbor between the interface on which we want to approach the flux but not on some of its faces. The second case is that the cell does not have nor neighbors associated with the considered face but also between some of its faces. Our idea is to construct the artificial points by considering the centroids of some faces. We present in the following some specific cases.

1. **Case 1: The neighbor cell is available**
   For example in the configuration shown in Figure 3 (Case 1-a), we replace $\mathbf{X}_a$ or $\mathbf{X}_b$ by the midpoint of the face which is at the top or in lower part of the face where we want to approach the flux. Or in another situation like that shown in Figure 3 (Case 1-b), we replace $\mathbf{X}_a$ or $\mathbf{X}_b$ by the midpoint of the corresponding M_i sides.

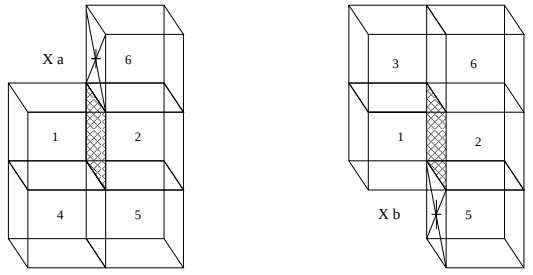

Case 1-a

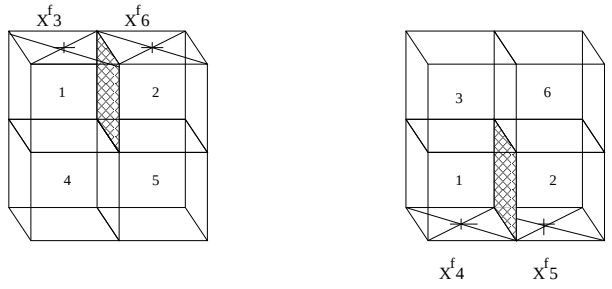

Case 1-b

Figure 3: Configuration with neighbor

2. **Case 2: The neighbor cell is not available**
   In the case shown in Figure 4 (Case 2-a), $\mathbf{X}_a$ is replaced by the midpoint of

the face on which we want to approach the flux (respectively $\mathbf{X}_b$). For the case shown in Figure 4 (Case 2-b), $\mathbf{X}_a$ and $\mathbf{X}_b$ are respectively replaced by the midpoint of the faces which are at the top and in lower part of the face.

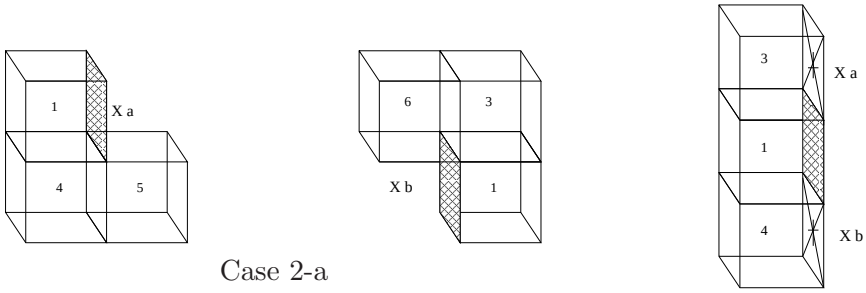

Case 2-a Case 2-b

Figure 4: Configuration without neighbor

Remark 1. The construction of $\mathbf{X}_c$ and $\mathbf{X}_d$ is same as for $\mathbf{X}_a$ and $\mathbf{X}_b$ presented above.

4. Numerical Validation

4.1. Convection Validation Tests

To validate the convection part using the general state law (2), we investigate the widely used tests in the literature: the shock tube problem introduced by Gary [13] and the Lax test in Lax [19] in their 3D version. The considered mesh is 101×11×101 and the domain is the unit cube. The time step is calculated using the CFL condition: $\max\limits_{1\leq k\leq 3} |\lambda_k| \dfrac{\triangle t}{\triangle x} < 1$ (λ_k is the wave-speed, $\triangle x = \min |F_{i^+} - F_{i^-}|$, F_{i^+}, F_{i^-} are two adjacent faces of the cell M_i). At $t = 0$ datum are respectively:

$$\text{shock tube:} \quad (\rho, \mathbf{u}, p) = \begin{cases} 1.0,\ (0,0,0),\ 1.0 & \text{if} \quad x < 0.5, \\ 0.1,\ (0,0,0),\ 0.125 & \text{if} \quad x > 0.5, \end{cases} \tag{15}$$

$$\text{Lax test:} \quad (\rho, \mathbf{u}, p) = \begin{cases} 0.445,\ (0,0,0),\ 3.528 & \text{if} \quad x < 0.5, \\ 0.5,\ (0,0,0),\ 0.571 & \text{if} \quad x > 0.5. \end{cases} \tag{16}$$

Figures 5 and 6 represent the numerical solution in the middle of the cube and one can see that the expected results are reproduced. However it is clear that some numerical diffusion appears mainly on the rarefaction. This is related to Godunov scheme.

The shock tube problem and the Lax test were conducted with the conditions of symmetry on the boundary, in the following the resolution of the half Riemann problem is tested. We use the initial datum (15) and various boundaries conditions on the velocity given by (17) in order to obtain different wave types. Figures 7 and 8 shows the horizontal velocity profiles and one can see clearly the effect of the boundary condition

$$\mathbf{u}_b = \begin{cases} (-0.2,0,0)_a,\ (-0.2,0,0)_b,\ (-0.9,0,0)_c,\ (-0.9,0,0)_d & \text{if} \quad x = 0, \\ (-0.5,0,0)_a,\ (0.5,0,0)_b,\ (-0.5,0,0)_c,\ (0.5,0,0)_d & \text{if} \quad x = 1. \end{cases} \tag{17}$$

4.2. Diffusion Validation Tests

The diffusion part presented in Section 2 is composed of two systems: the momentum diffusion (3) (vector case) and heat diffusion (4) (scalar case). The presented scheme is tested for the two cases.

4.2.1. Scalar Case

For this test, we use the heat equation (18). The considered domain is $\Omega = [0, L] \times [0, L] \times [0, L]$ with boundary $\partial\Omega$ divided in to three parts defined as follow:

$$\Gamma_1 = \left\{x = 0,\ (y,z) \in \mathbb{R}^2\right\}\ ,\ \Gamma_2 = \left\{x = L,\ (y,z) \in \mathbb{R}^2\right\} \text{ and } \Gamma_3 = \partial\Omega \setminus \Gamma_1 \cup \Gamma_2.$$

$$\begin{cases} \rho C_v \dfrac{\partial u}{\partial t} - k \triangle u = 0 & \text{in} \quad [0,T] \times \Omega, \\ u(x = 0, y, z, t) = u_1 & \text{on} \quad \Gamma_1, \\ u(x = L, y, z, t) = u_2 & \text{on} \quad \Gamma_2, \\ u = u_1 + \frac{x}{L}(u_2 - u_1) & \text{on} \quad \Gamma_3. \end{cases} \tag{18}$$

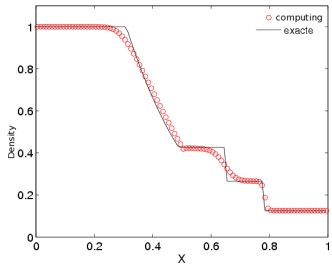

Density

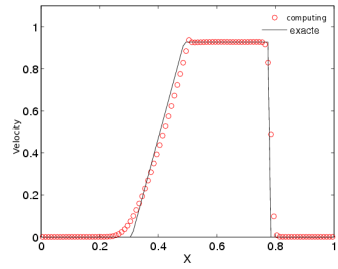

Velocity: u_x

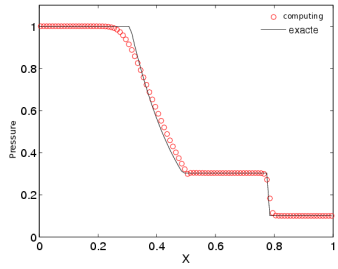

Pressure

Figure 5: 3D Gary A. Sod test: Y=0.5, Z=0.5, CFL=0.9, time=0.15

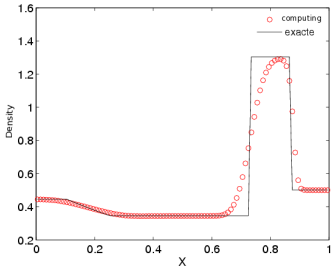

Density

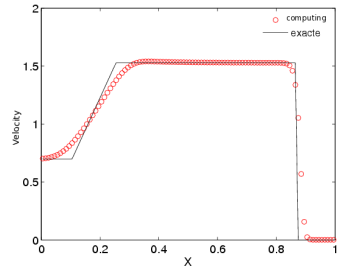

Velocity: u_x

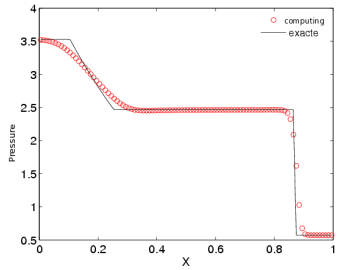

Pressure

Figure 6: 3D Lax P D test: Y=0.5, Z=0.5, CFL=0.9,time=0.15

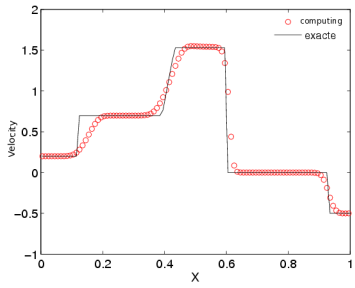

shock-shock (a)

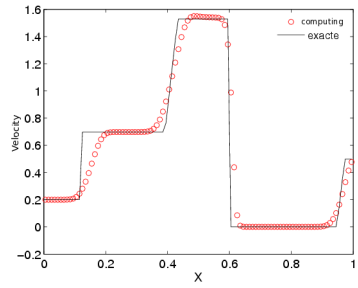

shock-rarefaction (b)

Figure 7: Velocity profile (Gary A. Sod test): Y=0.5, Z=0.5, CFL=0.9

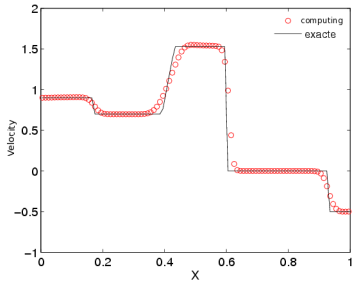

rarefaction-shock (c)

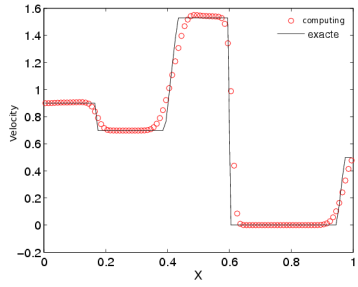

rarefaction-rarefaction (d)

Figure 8: Velocity profile (Gary A. Sod test): Y=0.5, Z=0.5, CFL=0.9

The exact solution is given by:

$$u^{\mathrm{ex}}(x,y,z,t) = \exp^{-\frac{12\pi}{L^2}\frac{k}{\rho C_v}t} \sin\frac{2\pi x}{L}\sin\frac{2\pi y}{L}\sin\frac{2\pi z}{L} + u_1 + \frac{x}{L}(u_2 - u_1).$$

The plane cut of the different meshes is given in figure 9. We represent in Figures 10 the exact solution u^{ex} and the computed solution u^{comp} on two structured meshes $10 \times 10 \times 10$ and $20 \times 20 \times 20$. The solutions computed on the unstructured meshes (Figure 9) are shown in Figure 11. The obtained results are similar which give a good accuracy of the our presented scheme.

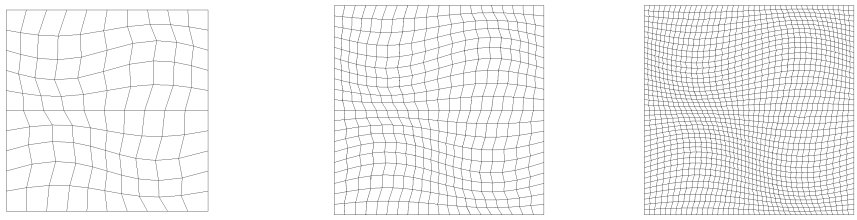

Figure 9: 2D cut of meshes: Mesh1 (Left), Mesh2 (Center), Mesh3 (Right)

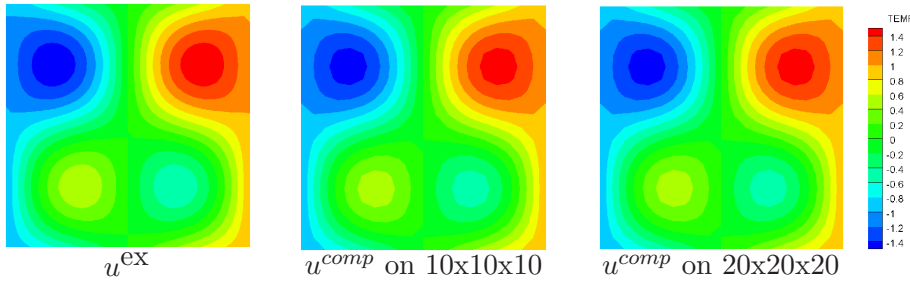

u^{ex} u^{comp} on 10x10x10 u^{comp} on 20x20x20

Figure 10: Tests on structured meshes

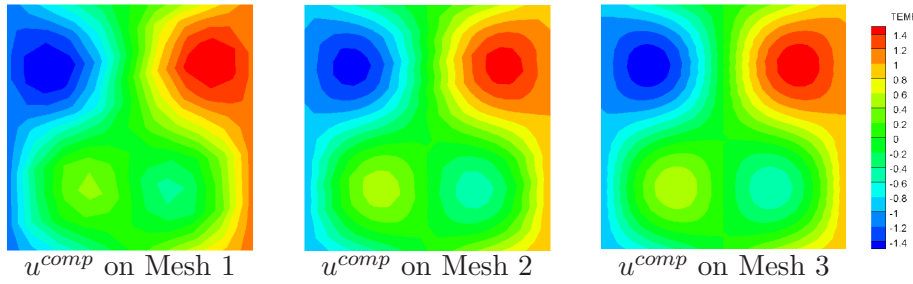

u^{comp} on Mesh 1 u^{comp} on Mesh 2 u^{comp} on Mesh 3

Figure 11: Tests on unstructured meshes

4.2.2. Vector Case

In this part we study the error made by our approximation on a vector variable. The considered domain is the same like in the scalar test but a homogeneous Dirichlet boundary condition is used. We consider the following problem:

$$\rho\frac{\partial \mathbf{u}}{\partial t} - \mu\triangle\mathbf{u} - (\frac{\mu}{3} + \lambda)\nabla(\nabla\cdot\mathbf{u}) = 0,$$

and the exact solution is given by

$$\mathbf{u}(t,x,y,z) = \exp(-\frac{4\pi^2(3\mu+\frac{\lambda}{3})t}{L^2})\sin(\frac{2\pi x}{L})\sin(\frac{2\pi y}{L})\sin(\frac{2\pi z}{L})\tilde{\mathbf{e}}_{\mathbf{1}}.$$

The numerical relative error is represented in Figure 12 for various time steps (right) and meshes (left) where h is computed like in the convection resolution by $h = \min|F_{i+} - F_{i-}|$, F_{i+}, F_{i-} are two adjacent faces of the cell M_i).

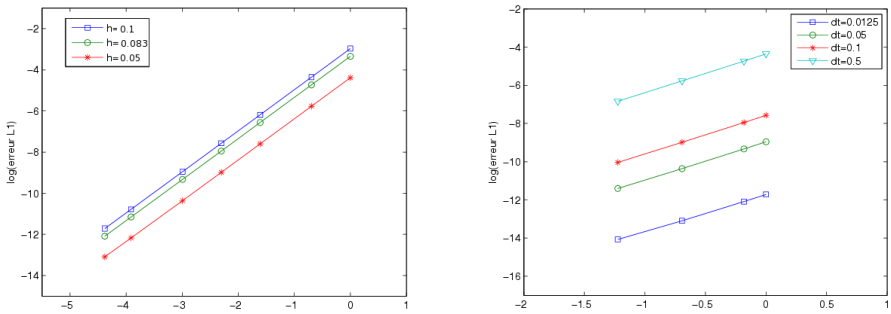

$\log(\triangle t)$ $\log(h)$

Figure 12: Relative error

4.3. The Natural Convection Test

To validate the numerical method presented in this work to solve the 3D compressible Navier-Stokes system, we present the natural convection numerical test. The domain and the used mesh are presented in Figure 13-a). For the boundary conditions, the velocity is taken homogeneous and a temperature gradient is imposed between the left and right ($\theta_c = 330$ and $\theta_h = 340$) and $\frac{\partial\theta}{\partial\mathbf{n}} = 0$ on the rest of the boundary (adiabatic). In time one can see the evolution of

the temperature and the velocity through a recirculation of the fluid induced by the temperature gradient between the two vertical sides. This instability depends on the dimensionless Rayleigh number (Ray). Figures 13-15 show the obtained results for various Rayleigh numbers $Ray = 10^3$, 10^4 and 10^5. This results are similar to that presented in the benchmark solutions in Jones et al [17].

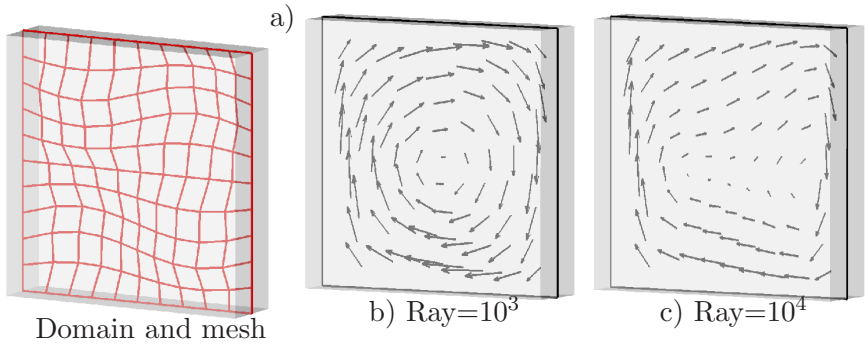

Figure 13: Computed velocity field

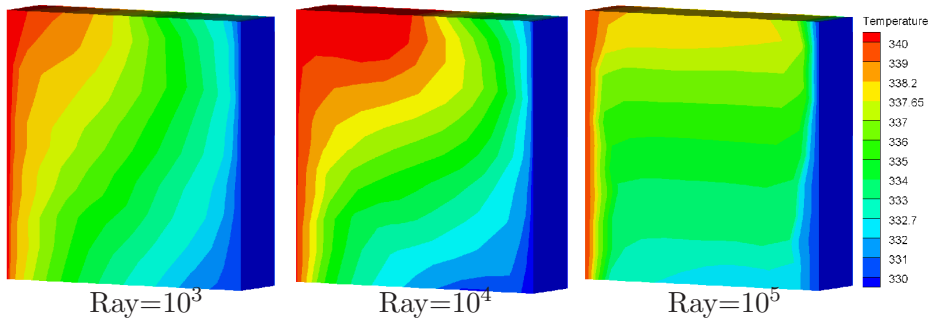

Figure 14: Contour of the computed temperature

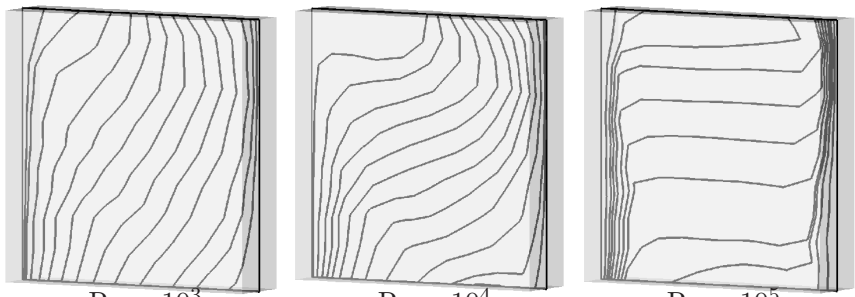

Figure 15: Isolines of the computed temperature

References

[1] H. Abboud, T. Sayah, A full discretization of the time-dependent Navier-Stokes equations by a two-grid scheme, *Math. Modelling and Numerical Analysis*, **42**, No 1 (2008), 141-174.

[2] R. Abgrall, R. Saurel, A simple method for compressible multiphase flows, *SIAM J. Sci. Comput.*, **21**, No 3 (1999), 1115-1145.

[3] N. Andrainov, S.W. Richard, A simple method for compressible multiphase mixture and interfaces, *Rapport de Recherche INRIA*, **RR-4247** (2001).

[4] C. Bernardi, Y. Maday, *Approximation spectrales pour les problèmes aux limites elliptiques*, Springer-Verlag, Paris (1992).

[5] S. Boivin, F. Cayré and J.M. Hérard, A finite volume method to solve the Navier-Stokes equations for incompresible flows on unstructured meshes, *Int. J. Therm. Sciences*, **39** (2000), 806-825.

[6] S. Boivin, J.M. Hérard and S. Perron, A finite volume method to solve the 3D Navier-Stokes equations on unstructured colocated meshes, *Computers and Fluids*, **33**, No 10 (2004), 1305-1333.

[7] A.J. Chorin, Numerical solution of the Navier-Stokes equations, *Math. of Computations*, **22** (1968), 745-762.

[8] K. Domelevo, P. Omnes, A finite volume scheme for the laplace equation on almost arbitrary two-dimensional grids, *Math. Modelling and Numerical Analysis*, **39**, No 6 (2005), 1203-1249.

[9] G. Edwige, P.A. Raviart, *Numerical Approximation of Hyperbolic Systems of Conservation Laws*, Collection Applied Mathematical Sciences 118, Springer-Verlag, New York (1996).

[10] R. Eymard, T. Gallouët and R. Herbin, *Finite Volume Methods*, In: *Handbook of Numerical Analysis*, Vol. 7 (Eds. P.G. Ciarlet, J.L. Lions), North Holland (2000), 713-1020.

[11] R. Eymard, T. Gallouët and R. Herbin, A cell-centred finite volume approximation for anisotropic diffusion operators on unstructured meshes in any space dimension, *IMA J. of Numer. Analysis*, **26** (2006), 326-353.

[12] I. Faille, A control volume method to solve an elliptic equation on two-dimensional irregular mesh, *Comp. Methods in Appl. Mech. and Eng.*, **100** (1992), 275-290.

[13] A.S. Gary, A survey of several finite difference methods for systems of nonlinear hyperbolic conservation law, *J. of Comp. Physics*, **2** (1978), 1-31.

[14] V. Girault, P.A. Raviart, *Finite Element Approximation of the Navier-Stokes Equations*, Lecture Notes in Math., 749, Springer, Berlin (1981).

[15] R. Glowinski, O. Pironneau, Finite element methods for Navier-Stokes equations, *Ann. Rev. Fluid Mech.*, **24** (1992), 167-204.

[16] M.Y. Hussaini, C. Canuto, A. Quarteroni and T.A. Zang, *Spectral Methods in Fluid Dynamics*, Springer-Verlag, Berlin (1988).

[17] I.P. Jones, P. Thompson, *Numerical Solutions for a Comparison Problem on Natural Convection in Enclosed Cavity*, Report 9955, Computer Science and Sys. Division AERE, Harwell, England, January (1981).

[18] K. Kirkkörrü, M. Uygun, Numerical solution of the Euler equations by finite volume methods: central versus upwind schemes, *J. of Aeronatics and Spaces Tech.* **2**, No 1 (2005), 47-55.

[19] P.D. Lax, Weak solutions of non-linear hyperbolic equations and their numerical approximation, *Comm. Pure and Appl. Math.*, **7** (1954), 159-193.

[20] P.D. Lax, *Hyperbolic Systems of Conservation Laws and Mathematical Theory of Schock Wave*, Conf. Board of the Math. Sciences-National Science Foundation (CBMS-NSF), Regional Conf. Series in Appl. Mathematics 11, SIAM, Philadelphia (1972).

[21] G. Manzini, A. Russo, A finite volume method for advection diffusion problems in convection-dominated regimes, *Comput. Methods Appl. Mech. Eng.*, **197** (2008), 1242-1261.

[22] P.D. Minev, L.J.P. Timmernans and F.N. Van De Vosse, An approximate projection scheme for incompressible flow using spectral elements, *Int. J. Numer. Methods Fluids*, **22** (1996), 673-688.

[23] O. Pironneau, S. Huberson, Characteristique-Galerkin and the particular method for convection-diffusion equation on the Navier-Stokes equations, *Lecture in Applied Mathematics*, **28**, (1991), 547-565.

[24] D. Serre, *Système de lois de conservation, I*, Arts and Sciences, Paris-New York-Amsterdam (1996).

[25] R. Temam, Sur l'approximation de la solution des equations de Navie-Stokes par la méthode des pas fractionnaires, II, *Arch. Rat. Mech. Anal.*, **33** (1969), 377-385.

[26] R. Temam, *Navier-Stokes Equations*, North-Holland, Amsterdam (1984).

[27] E.F. Toro, *Riemann Solvers and Numerical Methods for Fluid Dynamics*, Springer, Berlin-Heidelberg-New York (1997).